Published in final edited form as:
Cell. 2012 January 20; 148(1-2): 362–375. doi:10.1016/j.cell.2011.11.060.

Computational modeling of pancreatic cancer reveals kinetics of metastasis suggesting optimum treatment strategies

Hiroshi Haeno[1,*], **Mithat Gonen**[2,*], **Meghan B. Davis**[3], **Joseph M. Herman**[3,4], **Christine A. Iacobuzio-Donahue**[3,5,+], and **Franziska Michor**[1,+]

[1]Department of Biostatistics and Computational Biology, Dana-Farber Cancer Institute, and Department of Biostatistics, Harvard School of Public Health, Boston, MA 02115

[2]Department of Biostatistics and Epidemiology, Memorial Sloan-Kettering Cancer Center, New York, NY 10065

[3]The Sol Goldman Pancreatic Cancer Research Center, The Johns Hopkins Hospital, Baltimore, MD 21231

[4]Department of Radiation Oncology and Molecular Radiation Sciences, The Johns Hopkins Hospital, Baltimore, MD 21231

[5]Departments of Pathology, Oncology and Surgery, The Johns Hopkins Hospital, Baltimore, MD 21231

SUMMARY

Pancreatic cancer is a leading cause of cancer-related death, largely due to metastatic dissemination. We investigated pancreatic cancer progression by utilizing a mathematical framework of metastasis formation together with comprehensive data of 228 patients, 101 of whom had autopsies. We found that pancreatic cancer growth is initially exponential. After estimating the rates of pancreatic cancer growth and dissemination, we determined that patients likely harbor metastases at diagnosis and predicted the number and size distribution of metastases as well as patient survival. These findings were validated in an independent database. Finally, we analyzed the effects of different treatment modalities, finding that therapies which efficiently reduce the growth rate of cells earlier in the course of treatment appear to be superior to upfront tumor resection. These predictions can be validated in the clinic. Our interdisciplinary approach provides insights into the dynamics of pancreatic cancer metastasis and identifies optimum therapeutic interventions.

INTRODUCTION

Pancreatic cancer is the fourth-leading cause of cancer death and one of the most aggressive malignancies in humans, with a five-year relative survival rate of only 5% (Jemal et al., 2010). Pancreatic cancer often develops without early symptoms, and therefore most patients are diagnosed with metastatic disease. Treatment options including surgery, radiation, and chemotherapy can prolong survival and/or relieve symptoms in many patients,

[+]Authors for correspondence. Rapid autopsy, ciacobu@jhmi.edu; Mathematical modeling, michor@jimmy.harvard.edu.
[*]These authors contributed equally to this work.

but rarely lead to a cure (Hidalgo, 2010; Stathis and Moore, 2010). Until recently, it was unknown if the poor survival of pancreatic cancer patients was due to a delay in diagnosis or to early metastatic dissemination during the clonal evolution of pancreatic cancer. However, by applying high-throughput genetic analyses to paired primary and metastatic pancreatic cancer tissues, recent findings indicate that up to seven years are required for the development of metastatic subclones within a primary carcinoma after it has formed, and an additional 2–3 years before these subclones disseminate, leading to patient death. These findings support the notion that metastasis is a late event in the clonal evolution of this disease (Campbell et al., 2010; Yachida et al., 2010). In this regard, the growth dynamics of pancreatic cancer follows a linear progression paradigm similar to that described for other tumor types, and thus is a useful model system for understanding the dynamics of metastasis formation in general.

The genetic features of pancreatic cancer have been explored in detail and indicate that telomeric shortening and activating mutations in *KRAS* are among the earliest and most pervasive alterations in pancreatic carcinogenesis (Hruban et al., 2000; Iacobuzio-Donahue et al., 2011; van Heek et al., 2002). These alterations are followed by inactivating mutations in the *CDKN2A* tumor suppressor gene in the mid-stage, and in the *TP53* and *SMAD4* tumor suppressor genes in the late stage of carcinogenesis (Iacobuzio-Donahue et al., 2011). Mutations in a variety of other genes such as *BRCA2, MLL3, TGFBR1/II* and *MKK4* may also occur, albeit at a much lower frequency (Iacobuzio-Donahue et al., 2011; Jones et al., 2008). Evaluation of the temporal sequence of these alterations further indicates that the majority, if not all, can be classified as founder mutations, i.e. those mutations present in the clonal population of cells within an intraductal precursor lesion that founded the infiltrating carcinoma (Yachida et al., 2010). Indeed, the vast majority of deleterious mutations and rearrangements in pancreatic cancer are now known to occur during intraductal carcinogenesis (Campbell et al., 2010; Stephens et al., 2011; Yachida et al., 2010). While less well understood, epigenetic alterations may also occur during carcinogenesis, leading to changes in gene expression of a variety of biomarkers (Sato and Goggins, 2006).

Beyond carcinogenesis, the molecular mechanisms that promote the metastatic spread of pancreatic cancer are less clear. The fact that the vast majority of disseminated pancreatic cancer cells do not form metastases (Nguyen et al., 2009), and that a subset of patients have no observable pancreatic metastases post-mortem despite similar clinicopathologic features as patients who do develop metastatic failure (Iacobuzio-Donahue et al., 2009), indicates that the development of metastatic disease requires the acquisition of one or more (epi)genetic events that may promote survival of disseminated cells within the circulation and/or target organ sites (Cameron et al., 2000; Luzzi et al., 1998; Nguyen et al., 2009; Nguyen et al., 2007; Polyak and Weiberg, 2009; Saha et al., 2001; Valastyan et al., 2009). Whether this (epi)genetic event occurs during intraductal carcinogenesis or during clonal evolution beyond formation of the carcinoma is uncertain. However, a study of the patterns of failure in patients with pancreatic cancer indicated that genetic inactivation of *SMAD4* during carcinogenesis, and hence dysregulation of canonical TGFβ signaling, is highly correlated with subsequent distant metastatic failure (Iacobuzio-Donahue et al., 2009). This finding suggests that loss of *SMAD4* during pancreatic carcinogenesis represents a major and perhaps initial pro-metastatic event for this tumor type, upon which subsequent events are superimposed (Iacobuzio-Donahue et al., 2009).

In addition to studies addressing the mechanisms by which pancreatic cancers gain metastatic ability, there is the need to understand the growth dynamics of pancreatic cancer and its metastases in association with systemic treatments. This is critical to know because, until early detection of pancreatic cancer becomes routine, most patients will likely continue to be diagnosed with advanced disease (Hidalgo, 2010; Stathis and Moore, 2010). For this

reason, high quality datasets derived from rapid autopsy participants allow an unprecedented documentation of metastatic burden from the time of diagnosis to death (Embuscado et al., 2005; Liu et al., 2009; Shah et al., 2004; Yachida et al., 2010). Here we utilize one of these highly unique patient datasets derived from a rapid autopsy program for patients with pancreatic cancer, together with a mathematical framework of pancreatic metastasis development, to understand the growth dynamics of cancer metastasis in the setting of commonly used anti-cancer therapies. This model is subsequently validated using a uniform cohort of patients who underwent curative resection of their pancreatic cancer followed by adjuvant chemotherapy and radiation therapy. Our approach is then used to identify optimum therapeutic interventions, which can be tested in the clinic. This work is part of an ongoing effort to analyze cancer metastases using mathematical and computational techniques (Andasari et al., 2011; Chauviere et al., 2010; Dingli et al., 2007; Jadhav et al., 2007; Klein and Holzel, 2006; Michor et al., 2006; Quaranta et al., 2008; Sherratt, 2001) and provides new insight into the complexity of metastatic dissemination as well as suggests optimal treatment strategies for patients diagnosed with this devastating disease.

RESULTS

Tumor size and metastatic burden of 228 pancreatic cancer patients

We utilized two independent databases for a combined number of 228 pancreatic cancer patients. The first database contains information on 101 pancreatic cancer patients who consented for autopsy in association with the Gastrointestinal Cancer Rapid Medical Donation Program (GICRMDP) at Johns Hopkins and died between October 2006 and February 2011 (Iacobuzio-Donahue et al., 2009; van Heek et al., 2002) this database is referred to the “autopsy cohort” (Table 1, Supplemental Table S1). Dates of diagnoses ranged from May 1995 to November 2010. For each patient, data on the primary tumor size and metastatic burden at diagnosis and at autopsy were recorded (Fig. 1a). In addition, at least one intermediate evaluation of the primary tumor, local and distant recurrence as well as metastases was available. Many patients had numerous metastatic tumors at the time of autopsy, and the metastatic burden was categorized into one of three classes: less than 10 metastases, 10–99 metastases, and more than 100 metastases.

The median age at diagnosis of these 101 patients was 64 (first and third quartiles: 55 and 71). The median size of the primary tumor was 3.7 cm (first and third quartiles: 2.8 and 4.2). Sixty-one patients (60%) had no evidence of metastases at diagnosis. The median size of the largest metastatic tumor in patients with metastatic disease at diagnosis was 2 cm (first and third quartiles: 1.2 and 3.0). The primary tumor was surgically removed in 26 patients (26%). At autopsy, nine patients (9%) did not have a detectable primary tumor and for those who had a detectable primary tumor at autopsy, the median size was 4.8 cm (first and third quartiles: 4 and 6). Fourteen patients (14%) had no metastatic deposits at autopsy, 19 (19%) had 1–10, 30 (30%) had 11–100, and 38 (37%) had more than 100 metastatic tumors. The diameters of largest metastases ranged from 0.5 to 14 cm with a median of 2.7 cm (first and third quartiles: 2 and 4). The median survival was significantly different (p-value < 0.0001) between those who underwent surgical resection of the primary tumor (24.5, first and third quartiles: 14.8 and 34.7 months, n=26) and those who did not (8.4, first and third quartiles: 4.5 and 16.8 months, n=75).

Using the 47 patients who had at least one intermediate time point between diagnosis and autopsy, we compared the fit of linear and exponential growth models of primary and metastatic tumors. The exponential model had a better fit than the linear model in 71% of the cases, with a median R^2 of 0.63 (0.24–0.88). Other growth models such as a logistic model did not converge for most patients, due to sparsity of the data.

The second database from Johns Hopkins Hospital contained information on 127 pancreatic cancer patients who received curative surgical resection between January 1994 and December 2008; this database is referred to the "adjuvant cohort" (Table 1). The median age was 61 (first and third quartiles: 56–68) and 51 (41%) of the patients were women. At the time of analysis, 89 (71%) patients were dead. The size of the primary tumor at the time of surgical resection ranged from 0.7 cm to 9.5 cm with a median of 3 cm (first and third quartiles: 2.5 and 4). Fifty (39%) of the primary tumors were poorly differentiated and seventy-seven (61%) had margin-negative resections. Fifty (39%) of the tumors had vascular invasion and 98 (78%) had perineural invasion. All patients received adjuvant chemotherapy and radiation therapy and had complete follow-up and available data on patterns of failure. A majority (84%) received 5-FU based chemoradiation while gemcitabine (16%) was also used as the backbone for chemoradiation. The median follow-up was 78 months and median overall survival was 21.0 months. Thirty-one developed a local recurrence in the tumor bed while 64 developed distant metastases as a site of first failure. Patterns of failure (local, regional, and distant) and burden (quantitative) of disease were recorded until death.

A mathematical framework to investigate growth and dissemination

We designed a mathematical model of pancreatic cancer progression and dissemination to investigate the dynamics of cancer cell growth and metastasis, the survival of patients, and optimum intervention strategies. The model considers exponential expansion of pancreatic cancer cells starting from a single cell that has not yet evolved the ability to metastasize; this cell might, however, already have accumulated all necessary (epi)genetic alterations for proliferation. We chose an exponential model over other functional forms since the exponential model provided a better fit to the data as compared to a linear model (R^2 of 0.63, see above) and does not require as many data points to be reliably fit as some of the more complex models. In the context of our mathematical model, the cells follow a stochastic process: during each elementary time step, a cell is chosen proportional to fitness for reproduction, death, or export from the primary tumor to establish a metastatic colony elsewhere. Time is measured in numbers of cell divisions.

Cells that have not yet evolved the ability to metastasize are called type-0 cells (Fig. 1b). These cells divide at rate r and die at rate d per time unit. Initially, we consider metastatic ability to be a consequence of a single genetic or epigenetic change, for example the genetic inactivation of *SMAD4* (Hahn et al., 1996; Iacobuzio-Donahue et al., 2009; Nguyen et al., 2007; Polyak and Weinberg, 2009; Saha et al., 2001; Valastyan et al., 2009) this assumption will be relaxed in later sections. Such an (epi)genetic alteration occurs with probability u per cell division. Cells carrying the alteration are called type-1 cells. These cells divide at rate a_1 and die at rate b_1 per time unit. Once a type-1 cell has been produced, it has a certain probability of being exported from the primary tumor to attempt the establishment of metastases elsewhere. The integrated rate of leaving the primary site and founding a new colony at a distant site is denoted by q (Fig. 1b). Mutation and dissemination are unlikely to occur at the same time but instead are likely separated in time.

The relative fitness of type-1 cells as compared to type-0 cells is given by $\alpha_1 = (a_1 - b_1 - q)(r - d)$ since an increased rate of export, q, contributes to the loss of cells from the primary tumor and hence leads to a selective disadvantage of type-1 cells in that environment. If $\alpha_1=1$, then the fitness of type-1 cells is neutral as compared to that of type-0 cells and the metastasis-enabling mutation does not confer an advantage or disadvantage to the cell in the primary tumor. If $\alpha_1>$ – either through an increased growth rate or a decreased death rate of type-1 cells, then these cells have a fitness advantage; and if $\alpha_1<$ – either through a decreased growth rate, an increased death rate or a sufficiently large rate of export of type-1 cells, then they have a fitness disadvantage as compared to type-0 cells in the primary tumor.

Once a type-1 cell has migrated to a distant site, it initiates exponential growth with division rate a_2 and death rate b_2 per time unit. The relative fitness of type-2 cells as compared to type-1 cells is given by $\alpha_2 = (a_2 - b_2)\ (a_1 - b_1 - q)$. Again, if $\alpha_2 = 1$, then the fitness of type-2 cells is neutral, if $\alpha_2 >$, it is advantageous, and if $\alpha_2 <$, it is disadvantageous as compared to the fitness of type-1 cells in the primary tumor.

The total number of tumor cells (including all three types) at diagnosis is denoted by M_1, and the total number of tumor cells at autopsy is given by M_2. Here diagnosis refers to the initial detection of the tumor when the patient is first admitted to the hospital, and autopsy refers to the time of patient death when the tumor burden is assessed and the cause of death is determined. We expect that all three cell types contribute to the size at diagnosis since in rare cases, metastatic disease with unknown primary is diagnosed, where only type-2 cells can be detected (Ayoub et al., 1998). Once the tumor has been diagnosed with a population size of M_1, there are four options in the mathematical framework, which in the clinic depend on a host of other factors such as patient age and co-morbidities: (i) there may be no treatment; (ii) the patient may receive surgery, which removes a fraction ε of the primary tumor; (iii) the patient may undergo chemotherapy or chemoradiation, which reduces the growth rate of all cells by a factor of γ; or (iv) the patient may receive surgery and chemotherapy or chemoradiation.

This stochastic mathematical model serves to investigate the probability that metastases are present within a patient at a particular time during tumorigenesis, the total number of cancer cells, the effect of chemotherapy or chemoradiation and resection on these quantities, and the survival time of cancer patients. Analytic approximations for those quantities are shown in the Experimental Procedures section. With these quantities, we then estimated the mutation rate (u) and metastasis rate (q) by minimizing the deviations between the patient data on the numbers of metastatic sites and metastatic cells and the corresponding predictions obtained using the formulas. This approach could only be performed utilizing the autopsy patient cohort for whom detailed information of metastatic burden after death was available. Using these estimates, we then predicted the risk of metastasis at diagnosis as well as the expected number and size of metastatic sites and patient survival in both databases (autopsy and adjuvant cohorts). Finally, we investigated the effects of different treatment modalities on patient survival.

Growth kinetics of primary and metastatic tumors

We first investigated the correlations between primary and metastatic tumor sizes at diagnosis and autopsy as well as their growth rates utilizing the autopsy patient cohort (Table 2). In general, primary tumor-related variables were significantly correlated with each other and metastasis-related variables were significantly correlated with each other. Of note, tumor growth was slower for primary tumors that were larger at diagnosis. This effect is not a function of primary tumor removal, as the partial correlation between growth of the primary and size at diagnosis was −0.25 (p-value = 0.03, partialing out primary removal). In the adjuvant cohort, all patients underwent surgery so the corresponding partial correlation could not be estimated, but the correlation between size at resection and local growth rate was insignificant (correlation coefficient −0.07, p-value = 0.73).

Survival times were calculated from diagnosis to death, and growth rates of primary and metastatic tumors were computed using our exponential growth model. For some patients, no tumor was detected at a given location (primary or metastatic) at a given time (diagnosis, intermediate evaluations, or autopsy). We imputed a tumor size of 0.1 cm for those time points, based on estimates of the minimal size of radiographically detectable local and metastatic tumors (MSKCC gastroenterologists, personal communication). This choice was further supported by the fact that the smallest measured tumor anywhere at any time point in

our data was 0.2 cm. Table 2 and Figure S1a present the correlations between tumor-related variables and survival. Both the size of the largest metastasis at diagnosis and the growth rate of metastatic tumors were significantly correlated with survival (in each case, p-value < 0.05). We also tested the sensitivity of our results for variations in the assumption of a 0.1 cm diameter for undetected metastases. In Supplemental Table S2, we reproduced Table 2 while using 0.2 and 0.05 cm as the minimally detectable tumor sizes with radiographic imaging. Most of our conclusions remained unchanged, suggesting robustness of our findings.

We then estimated the model parameters using the autopsy patient cohort (see Supplemental Material and Supplemental Table S2c). The coefficients in Table S2c are on a multiplicative scale; for example, surgical removal of the primary almost doubles predicted survival ($e^{0.632}$=1.88) when growth rates and size of the largest metastatic tumor at diagnosis were held constant. One unit increase in either the primary or the metastatic growth rate (other factors kept constant) decreased predicted survival by approximately 22%, and one cm increase in the largest metastatic tumor decreased predicted survival by 32%. All of these factors were significantly associated with survival. This robust regression model had a good fit (R^2 = 0.41, AIC = 102.9) and approximately normally distributed residuals (Figures S1b and c).

Because of the multiple combination regimens used in the autopsy cohort, only limited analyses of treatment effects could be performed for this database. Forty-one (41%) of the patients in the autopsy cohort received chemotherapy only, while 45 received both chemotherapy and radiotherapy. Neo-adjuvant therapy was used in only two patients, while the rest of the treatments in the surgical patients were in the adjuvant setting. First-line treatment included gemcitabine in 56 of the 86 patients (65%) who received chemotherapy and 5-FU in 10 patients (12%).

The adjuvant cohort of patients, in contrast, did contain information about the use of chemotherapy following resection. In this patient cohort, all patients received adjuvant chemotherapy, with 84% receiving 5-FU based chemoradiation and 16% gemcitabine-based therapy. There was no difference between the survival profiles of patients receiving 5-FU or gemcitabine in the adjuvant setting (p-value = 0.68, Wilcoxon test).

The probability of metastases at diagnosis

We then utilized our mathematical framework to estimate the rate of accumulating one specific (epi)genetic alteration that enables cells to metastasize (u in our mathematical model) and the dissemination rate (q) by using information regarding the numbers of metastatic sites and metastatic cells at autopsy from the autopsy patient cohort. Figure 1c shows the log-scale deviations between the data and the predictions of the model (see Experimental Procedures) for a wide range of values of the mutation and dissemination rates, u and q. We identified the region of fit for these rates as $10^{-13} < u\,q < 10^{-9}$. We then further investigated the fit between data and theory in this parameter region (Fig. 1d) while using a constraint of the mutation rate, $10^{-8} < u < 10^{-4}$; this choice was made since experimental evidence suggests that the mutation rate per base per cell division is about 10^{-8} in genetically stable cells and about 10^{-4} in cells with microsatellite instability (Lengauer et al., 1997, 1998; Seshadri et al., 1987). Values of $u = 6.31 \cdot 10^{-5}$ and $q = 6.31 \cdot 10^{\cdot 7}$ were identified as the best combination of these parameters that minimize the deviations between data and theory (see Experimental Procedures for details of the parameter estimation).

Using our mathematical framework together with the estimated rates, we then investigated the probability that metastatic cells as well as cells with the potential to metastasize are

present at the time of diagnosis (Fig. 1e). Of note, we found that all patients are expected to harbor metastasis-enabled cells in the primary tumor at the time of diagnosis, even when the size of the primary tumor is small. Not all patients, however, are expected to present with metastatic disease at diagnosis (Fig. 1e). A patient with a primary tumor of 1 cm diameter, for example, has a probability of 28% of harboring metastases at the time of diagnosis; as the primary size increases to 2 and 3 cm, the risk of harboring metastases becomes 73% and 94%, respectively.

To validate the accuracy of the mathematical framework and the estimated parameter values, we tested the fit between the autopsy patient data and our model predictions with regard to the distribution of survival times, the size of the primary tumor, and the extent of metastatic disease at autopsy (Fig. 2). We obtained an accurate fit for these quantities, suggesting that our mathematical framework together with the estimated mutation and dissemination rates capture the dynamics of pancreatic tumor growth and metastasis formation exceptionally well.

We then sought to further validate our predictions in an independent database of pancreatic cancer patients who underwent curative resection (pancreaticoduodenectomy) and received adjuvant 5-FU or gemcitabine-based chemoradiation. We first validated the growth rate estimates obtained from the autopsy dataset using this adjuvant patient cohort, and observed agreement between the estimates (Fig. 3a). We then tested our predictions of survival times using the adjuvant cohort: we used the growth kinetics learned from the autopsy database to predict the distribution of survival times in the adjuvant database and obtained an excellent fit (Fig. 3b–d). Note that the variability in the patient data is due to the small number of patients for whom sufficient data was available (18, 28, and 22 patients for panels b, c, and d, respectively).

Treatment reducing tumor cell proliferation most effectively prolongs survival

After validating the accuracy of the mathematical model and the estimated parameter values in two independent databases, we utilized our mathematical framework to evaluate the effects of different treatment options on patient survival. This investigation was performed using the distributions of tumor sizes at autopsy and the growth rates of primary and metastatic tumors provided by the autopsy patient cohort, as well as the estimated mutation and dissemination rates. These quantities were then used to predict the effects of therapeutic options on disease outcomes (Fig. 4). We evaluated both resection and chemotherapy strategies for their effectiveness in attenuating tumor progression and prolonging survival. Interestingly, a reduction in the growth rate of both primary and metastatic tumor cells was more efficient in extending patient life expectancy than surgical resection (Fig. 4a and b, red curves). Surgical resection of the primary tumor, even if done efficiently such that 99.99% (i.e., no macroscopic disease left behind) of the primary tumor was removed, led to less promising results (Fig. 4a and b, blue curves). This finding indicates that a reduction in the growth rates of primary and metastatic tumors may be more effective in attenuating tumor growth than upfront surgical resection of the tumor mass since inevitably, a fraction of cells will remain and lead to exponential expansion of the tumor while the patient is recovering from surgery (average 4–12 weeks). As expected, therapeutic interventions that are initiated as soon as possible after diagnosis, and diagnostic tools that lead to earlier discovery of the tumor, are more effective than interventions that commence at a later time. Moreover, we investigated the effects of different treatment strategies on the number of metastatic sites at autopsy, the number of primary tumor cells, the number of metastatic tumor cells, and the number of metastatic tumor cells per site (Fig. 4c–j). The expected number of metastatic sites at autopsy increases with the administration of chemotherapy and decreases with resection, because slow tumor growth caused by drug therapy enhances the chance of metastatic events while resection decreases the number of primary tumor cells, which are the

underlying cause of metastatic events (Fig. 4c–d). Surgical resection decreases the number of primary tumor cells at autopsy (Fig. 4e–f). The number of metastatic cells at autopsy does not vary with different treatment options (Fig. 4g–h), implying that the number of metastatic cells is generally the determinant of death. Patients who receive chemotherapy tend to harbor smaller metastatic sites and those who receive tumor resection have large metastatic sites (Fig. 4i–j).

Figure 5 displays the effects of treatment delays both on the tumor volume and patient survival for a set of theoretical therapeutic interventions (see Experimental Procedures for details of the calculations). We found that early initiation of treatment effectively prolongs survival and that any treatment delay leads to a worse prognosis than earlier initiation of therapy, indicating that immediate suppression of tumor growth is essential for patient survival.

Additional factors related to patient outcome

We then estimated the cross-correlations of all clinical variables in the adjuvant patient cohort. There were significant correlations between the following pairs of variables: CAD and MI (correlation=0.56, $p<0.001$), CAD and HTN (0.29, 0.001), CAD and grade (0,23, 0.008) and PNI and grade (0.19, 0.032); these findings are in line with previously published results.

Finally, we identified important indices that forecast the prognosis of patients with statistical significance (Table S1b). As expected, tumor pathological grade was found to be a significant indicator of prognosis (p-value = 0.014). Moreover, we found that a high concentration of the tumor marker CA 19-9 before surgery (p-value = 0.005) and after surgery (p-value = 0.001) significantly indicates poor prognosis. None of the other correlations were significant.

Alternative model assumptions

To investigate the robustness of our findings to the assumption that a single (epi)genetic alteration is sufficient to confer metastatic ability to pancreatic cancer cells, we designed an alternative mathematical framework in which two alterations are necessary to gain such ability (Supplemental Material). The model considers exponential expansion of pancreatic cancer cells starting from a single cell that has not yet evolved the ability to metastasize. Again, the cells follow a stochastic process: during each elementary time step, a cell is chosen proportional to fitness for reproduction, death, or export from the primary tumor to establish a metastatic colony elsewhere. Cells that have not yet acquired the ability to metastasize are called types0 cells and accumulate the first alteration towards the metastatic phenotype with probability v_1 per cell division. Cells carrying this alteration are called type-s1 cells and accumulate the second alteration towards the metastatic phenotype with probability v_2 per cell division. Cells carrying two (epi)genetic alterations are called type-s2 cells and may be exported from the primary tumor to attempt the establishment of metastases elsewhere at rate q. Once disseminated, the cells are called type-s3 cells. Type-s0, -s1, -s2, and -s3 cells divide at rates r, s_1, s_2, and s_3 while they die at rates d, d_1, d_2, and d_3, respectively, per time unit. This model was used to investigate the dynamics of growth, dissemination, and treatment response of pancreatic cancer patients, both for genetically stable cells as well as tumors with genomic instability (Fig. S2–S7). Although we were unable to estimate both mutation rates as well as the dissemination rate from patient data, the main predictions of our framework remained consistent with this alternative modeling assumption (Fig. S2–S7). For instance, we again found that a reduction of the growth rate is more effective for prolonging patient survival than surgical removal of the primary tumor

(Fig. S2). Our conclusions are thus robust to the choice of the modeling framework to investigate pancreatic cancer growth and dissemination.

DISCUSSION

Computational modeling applied to well-annotated data derived from a large series of patients provides the unique opportunity to dissect the growth and dissemination dynamics of pancreatic cancer metastases. This approach indicated only a weak relationship between the growth characteristics of primary pancreatic cancers and their matched metastases. Of note, this observation is not simply explained by differences in therapeutic management, and is evidenced by large primary tumors (pT4 stage) without metastases at autopsy despite a long overall survival, and small primary carcinomas (pT1 stage) with concurrent widespread metastatic disease (Table S2c). Differences in growth kinetics of the primary and metastatic sites may be accounted for by inherent differences in the microenvironment (Nguyen et al., 2009; Talmadge and Fidler, 2010), by the extent of hypoxia (Lu and Kang, 2010), or by differences in the epigenetic or genetic features of the subclonal populations that gave rise to the distant metastases (Campbell et al., 2010; Yachida et al., 2010). These questions provide fertile ground for additional studies.

The biggest implication of this model is its predictions for timing of and type of clinical intervention that most effectively impact survival. For example, when investigating the correlation between the tumor-related variables and the survival time of patients (Table 2 and Fig. S1a), we found that both pancreatic tumor size at diagnosis/resection and growth rate of a pancreatic tumor shorten the patient's survival. We then estimated the rate of acquiring an (epi)genetic alteration that confers metastatic ability to tumor cells, u, and the dissemination rate of such cells, q, to be $u = 6.31 \cdot 10^{-5}$ per allele per cell division and $q = 6.31 \cdot 10^{-7}$ per time unit. The patient data, together with these rate estimates, were then used to predict the probability of metastatic disease at diagnosis, the number and size distribution of metastatic tumors, and the effects of particular treatment strategies on tumor volume and patient survival. Overall, our predictions suggest that chemotherapeutic agents capable of effectively reducing the growth rate of primary and metastatic tumors are most promising for prolonging survival of pancreatic cancer patients as compared to surgery alone. These predictions are testable in the laboratory and the clinic. Moreover, since our model predicts that most patients have metastatic disease at the time of diagnosis, upfront surgery which only influences local tumor progression is less effective than chemotherapy which can affect both local and distant tumor progression (Amikura et al., 1995; Yachida et al., 2010). Further, our model suggest that surgery serves only to debulk the overall tumor cell burden but does not fully eradicate it. By extension, this prediction also infers that earlier initiation of effective chemotherapeutic agents has a survival benefit by reducing the number of cells in the exponential growth stage (Fig. 5), a finding of tremendous clinical significance in light of the ongoing debates regarding neoadjuvant versus adjuvant treatment of resected pancreatic cancers (Hsu et al., 2010; Katz et al., 2009). Adjuvant chemotherapy and radiation after surgery has been shown to promote longer overall survival compared to patients who undergo surgery alone (Hsu et al., 2010). Of interest, recent data indicates that neoadjuvant therapy is associated with an even longer overall survival compared to adjuvant therapy in patients with resectable pancreatic cancer, in keeping with this possibility (Artinyan et al., 2011). The addition of neoadjuvant radiation therapy may slow tumor proliferation and prevent further metastases, while adjuvant radiation therapy may promote eradication of residual microscopic disease following surgery. However, our data suggests that aggressive full-dose systemic therapy is needed to suppress tumor proliferation. Therefore, if radiation therapy is used in the neoadjuvant/adjuvant setting, it should be delivered with full-dose aggressive chemotherapy (if possible) or the duration of radiation therapy needs to be minimized (stereotactic radiation) to allow for continuous chemotherapy

treatment in order to suppress tumor proliferation (Desai et al., 2009; Schellenberg et al., 2011).

In our statistical analyses, we did not consider a death bias because pancreatic cancer patients have a short expected survival time and are therefore unlikely to die from other causes. We also did not consider an autopsy consent bias since we did not find any evidence that patients who consented to a rapid biopsy had different characteristics than those who did not. Furthermore, in the autopsy database, we did not observe a significant difference in growth rates of tumors between patients that did and did not receive chemotherapy; this effect is likely due to the modest efficacy of currently available treatments (Neoptolemos et al., 2004; Neuhaus et al., 2008; Oettle et al., 2007) although it conceivably also stems from the small size of the autopsy cohort as well as the small number of patients receiving the same therapy. In the mathematical framework, we considered a common growth rate for all cells in the primary tumor – both cells that have not yet accumulated the alteration(s) conferring metastatic ability to cells, and metastases-enabled cells. The latter cells may have a different growth rate, which was not considered in the present study for clarity. Since detailed knowledge of these parameters is important for the determination of the accurate mathematical formulation and thus the dynamics of metastasis and identification of optimum treatment strategies, it is an important goal of the field to obtain these values from detailed kinetic studies of cancer cells. Finally, although the primary tumor sizes were obtained by pathology in the autopsy cohort and by imaging in the adjuvant cohort, we are confident that the values are comparable since based on data from our group and others (Arvold et al., 2011), the maximum tumor size on preoperative imaging is on average within 0–5 mm of the pathologic tumor size (Qui et al., manuscript in preparation).

Our work highlights the utility of a unique mathematical framework revealing the complex dynamics of the metastatic dissemination of pancreatic cancer cells and suggests that aggressive systemic therapy should be offered early after diagnosis regardless of the stage of the disease. Our findings also have implications for the investigation of other cancer types for which similar data can be obtained.

EXPERIMENTAL PROCEDURES

Mathematical expressions of metastatic properties

In order to estimate the metastatic mutation rate (u) and metastasis rate (q), we examined the deviations between the data of metastatic sites and metastatic cells and the predictions of our mathematical model. We used the data of the number of metastatic sites and metastatic cells from 23 patients whose tumors were not resected after diagnosis, who were treated with chemotherapy, and who had positive net growth rates. The formula for the expected number of metastatic sites is given by

$$E = \sum_{i=1}^{M_1-1} [A(i, t_i)(D_i - D_{i+1})] + E_0 + G \cdot E_1.$$

The first term on the right-hand side of the equation represents the expected number of new metastatic sites after diagnosis for the case in which type-1 cells exist at diagnosis. The second term represents the expected number of metastatic sites before diagnosis, and the third term denotes the expected number of new metastatic sites after diagnosis when no mutations occur before diagnosis.

Here

$$D_i = 1 - \exp\left[-\int_0^{k_i - h_i} rue^{(r(1-u)-d)v}\left(1 - \frac{b_1+q}{a_1}\right)dv\right].$$

We further have $h_i = \ln i/(a_1 - b_1 - q)$ and $k_i = \ln(M_1 - i)/(r(1-u) - d)$, as well as

$$\begin{aligned} A(i,t_i) &= \int_0^{t_i} qy(k)(1 - b_2/a_2')dk \\ &= \frac{y_0 q\left(e^{(a_1' - b_1 - q)t_i} - 1\right)\left(1 - b_2/a_2'\right)}{a_1' - b_1 - q} \\ &+ \frac{r' uqx_0(1 - b_2/a_2')}{r'(1-u) - d - a_1' + b_1 + q}\left(\frac{e^{(r'(1-u)-d)t_i} - 1}{r'(1-u) - d} - \frac{e^{(a_1' - b_1 - q)t_i} - 1}{a_1' - b_1 - q}\right), \end{aligned}$$

where $r' = r(1-\gamma)$, $a_1' = a_1(1-\gamma)$, $a_2' = a_2(1-\gamma)$, and

$$G = \exp\left[-\frac{M_1 u}{1 - d/r}\int_0^1 \frac{1 - (b_1+q)/a_1}{1 - [(b_1+q)/a_1]v^{\alpha_1}}dv\right],$$

where $\alpha_1 = (a_1 - b_1 - q)/(r - d)$.

The expected number of metastatic sites before diagnosis is given by

$$E_0 = \sum_{x=1}^{M_1 - 1} e^{-\beta(x-1)}\left(1 - e^{-\beta}\right)\left(qe^{(a_1 - b_1 - q)\tau_x}\left(1 - \frac{b_2}{a_2}\right)/(a_1 - b_1 - q)\right).$$

Here $\beta = (1 - (b_1 + q)/a_1)$ and τ_x is obtained from $xe^{(r-d)\tau_x} + e^{(a_1 - b_1 - q)\tau_x} = M_1$.

The expressions t_i is obtained from $(M_1 - i)(1-\varepsilon)e^{(r' - d)t_i} + i(1-\varepsilon)e^{(a_1' - b_1 - q)t_i} = M_2$.

The expected number of new metastatic sites after diagnosis for the case in which no mutations occur before diagnosis is given by

$$E_1 = \sum_{x = M_1(1-\varepsilon)}^{M_2 - 1} e^{-\beta(x-1)}\left(1 - e^{-\beta}\right)\left(qe^{(a_1' - b_1 - q)t_x'}\left(1 - \frac{b_2}{a_1'}\right)/\left(a_1' - b_1 - q\right)\right).$$

The expression t_x' in the equation is obtained from $xe^{(r' - d)t_x'} + e^{(a_1' - b_1 - q)t_x'} = M_2$.

The formula for the expected number of metastatic cells is given by

$$Z=\sum_{x=1}^{M_1-1}P(x)\int_0^{\tau_x}L(\sigma)z_a(t')d\sigma+\sum_{x=1}^{M_1-1}P(x)\exp\left[-\int_0^{\tau_x}qe^{(a_1-b_1-q)v}(1-b_2/a_2)dv\right]\int_0^{\tau'_x}L(\tau')e^{(a'_2-b_2)\kappa'_{x,\tau'}}d\tau',$$

where $P(x) = e^{-(x-1)\beta}(1-e^{-\beta})$

$$L(\sigma)=\exp\left[\frac{-\left(e^{(a_1-b_1-q)\sigma}-1\right)q}{a_1-b_1-q}\left(1-\frac{b_2}{a_2}\right)\right]\left(1-\exp\left[-qe^{(a_1-b_1-q)\sigma}\left(1-\frac{b_2}{a_2}\right)\right]\right),$$

and

$$L'(\tau')=\exp\left[-\int_0^{\tau'}qy_0e^{(a'_1-b_1-q)v}\left(1-\frac{b_2}{a'_2}\right)dv\right]\left(1-\exp\left[-qy_0e^{(a'_1-b_1-q)\tau'}\left(1-\frac{b_2}{a'_2}\right)\right]\right).$$

The expressions t', τ'_x, and $\kappa'_{x,\tau'}$ are respectively obtained from $x_0e^{(r'-d)t'}+y_0e^{(a'_1-b_1-q)t'}+z_0e^{(a'_2-b_2-q)t'}=M_2$, $x_0e^{(r'-d)\tau'_x}+y_0e^{(a'_1-b_1-q)\tau'_x}=M_2$, and $x_0e^{(r'-d)\left(\tau'+\kappa'_{x,\tau'}\right)}+y_0e^{(a'_1-b_1-q)\left(\tau'+\kappa'_{x,\tau'}\right)}+e^{(a'_2-b_2)\kappa'_{x,\tau'}}=M_2$. Moreover, $x_0=(1-\varepsilon)xe^{(r-d)(\sigma+\kappa_{x,\sigma})}$, $y_0=(1-\varepsilon)e^{(a_1-b_1q)(\sigma+\kappa_{x,\sigma})}$, and $z_0=e^{(a_2-b_2)\kappa_{x,\sigma}}$, and $\kappa_{x,\sigma}$ is obtained from $xe^{(r-d)(\sigma+\kappa_{x,\sigma})}+e^{(a_1-b_1-q)(\sigma+\kappa_{x,\sigma})}+e^{(a_2-b_2)\kappa_{x,\sigma}}=M_1$. The expression z_a is given by the differential equation $\frac{dz_a}{dt}=\left(a'_2-b_2\right)z_a$ with the initial condition, $z_a(0)=e^{(a_2-b_2)\kappa_{x,\sigma}}$. Here the number of primary tumor cells at autopsy is given by M_2-Z. For more details, see (Haeno and Michor, 2011).

Estimation of mutation and dissemination rates

The deviations between the data and formula are calculated by the following equation:

$$Dev=\sqrt{\prod_i\left(\ \ln[\,i\text{th data of the number of metastatic sites or cells}]-\ln[\,prediction(u,q,\gamma,r_i,a_{1i},a_{2i},d_i,b_{1i},b_{2i},M_{1i},M_{2i})]\ \right)^2}.$$

Here i is an index enumerating the patient data. In this analysis, we assumed that the net growth rates of type-0 cells and type-1 cells were the same, death rates of tumor cells (d, b_1, b_2,) were 100 times lower than division rate (r, a_1, a_2,), and the reduction of growth rate by chemotherapy (γ) was zero. We examined different values of the reduction of growth rates by chemotherapy and death rates and found little effect of such changes on the estimated regions of mutation and metastatic rates. The number of tumor cells in 1 cm^3 tumor bulk is considered to be a billion.

Reproduction of distributions of survival time and metastatic cells

For this analysis, we used estimated parameters of the net growth rate of the primary tumor (0.16 per month with variance 0.46) and metastases (0.58 per month with variance 2.72), mutation rate ($u = 6.31\cdot10^{-5}$), and dissemination rate ($q = 6.31\cdot10^{-7}$). The growth rates of primary and metastatic tumor cells with variance were obtained from the time series data of tumor size for all patients. We obtained the distribution of the total tumor cells in a base 10

logarithmic scale at autopsy as a normal distribution with mean 11.2 and variance 0.46 from the autopsy cohort. In the mathematical calculation, the number of tumor cells at autopsy followed this distribution. To obtain the survival time after diagnosis, we first consider the expected number of metastatic cells at diagnosis, given by

$$Z_d = \sum_{x=1}^{M_1-1} P(x) \int_0^{\tau_x} L(\sigma) e^{(a_2-b_2)\kappa_{x,\sigma}} \, d\sigma.$$

Then the survival time is given by

$$(M_1 - Z_d) e^{(r'-d)t_s} + Z_d e^{(a_2'-b_2)t_s} = M_2.$$

For more details, see (Haeno and Michor, 2011).

The effects of a delay in the initiation of therapy

We considered 100 cases in the mathematical model described above and for each case in which a patient develops a 3 cm tumor at diagnosis, we utilized the estimated mutation and metastatic rates as well as different primary and metastatic growth rates that follow normal distributions with the estimated mean and variance. Surgery removes 99.99% of primary tumor cells at time 0. We tested five scenarios: (i) no treatment after surgery, (ii) starting treatment immediately after surgery, (iii) starting treatment 2 weeks after surgery, (iv) starting treatment 4 weeks after surgery, and (v) starting treatment 8 weeks after surgery. Treatment reduces the growth rate of tumor cells by 70% in this analysis, which is derived from the validation of the model (Fig. 2 and 3). The number of tumor cells at death follows a normal distribution with mean 11.2 and variance 0.46 in a base 10 logarithmic scale. Survival time after surgery, t_s, is obtained from

$$(M_1 - Z_d) e^{(r-d)t_j} e^{(r'-d)(t_s-t_j)} + Z_d e^{(a_2-b_2)t_j} e^{(a_2'-b_2)(t_s-t_j)} = M_2,$$

where treatment starts at time t_j. The first term on the left-hand side represents the number of primary tumors and the second term represents the number of metastatic tumor cells after surgery.

Supplementary Material

Refer to Web version on PubMed Central for supplementary material.

Acknowledgments

The authors would like to thank the Michor lab and Georg Lübeck for helpful comments. This work was supported by National Institutes of Health grants CA106610 and CA62924 (CID), Pilot Funding from the Sol Goldman Pancreatic Cancer Research Center, the Michael Rolfe Pancreatic Cancer Foundation, the George Rubis Endowment for Pancreatic Cancer Research, the Joseph C. Monastra Foundation for Pancreatic Cancer Research, and The Alfredo Scatena Memorial Fund. Furthermore, we would like to acknowledge support from the National Cancer Institute's Physical Sciences-Oncology Center, U54CA143798 (HH, MG, FM).

References

Amikura K, Kobari M, Matsuno S. The time of occurrence of liver metastasis in carcinoma of the pancreas. Int J Pancreatol. 1995; 17:139–146. [PubMed: 7622937]

Andasari V, Gerisch A, Lolas G, South AP, Chaplain MA. Mathematical modeling of cancer cell invasion of tissue: biological insight from mathematical analysis and computational simulation. J Math Biol. 2011; 63:141–171. [PubMed: 20872264]

Artinyan A, Anaya DA, McKenzie S, Ellenhorn JD, Kim J. Neoadjuvant therapy is associated with improved survival in resectable pancreatic adenocarcinoma. Cancer. 2011; 117:2044–2049. [PubMed: 21523715]

Arvold ND, Niemierko A, Mamon HJ, Fernandez-Del Castillo C, Hong TS. Pancreatic Cancer Tumor Size on CT Scan Versus Pathologic Specimen: Implications for Radiation Treatment Planning. Int J Radiat Oncol Biol Phys. 2011; 80:1383–1390. [PubMed: 20708856]

Ayoub JP, Hess KR, Abbruzzese MC, Lenzi R, Raber MN, Abbruzzese JL. Unknown primary tumors metastatic to liver. J Clin Oncol. 1998; 16:2105–2112. [PubMed: 9626210]

Cameron MDSE, Kerkvliet N, Nadkarni KV, Morris VL, Groom AC, Chambers AF, MacDonald IC. Temporal progression of metastasis in lung: cell survival, dormancy, and location dependence of metastatic inefficiency. Cancer Res. 2000; 60:2541–2546. [PubMed: 10811137]

Campbell PJ, Yachida S, Mudie LJ, Stephens PJ, Pleasance ED, Stebbings LA, Morsberger LA, Latimer C, McLaren S, Lin ML, et al. The patterns and dynamics of genomic instability in metastatic pancreatic cancer. Nature. 2010; 467:1109–1113. [PubMed: 20981101]

Chauviere AH, Hatzikirou H, Lowengrub JS, Frieboes HB, Thompson AM, Cristini V. Mathematical Oncology: How Are the Mathematical and Physical Sciences Contributing to the War on Breast Cancer? Curr Breast Cancer Rep. 2010; 2:121–129. [PubMed: 21151486]

Desai S, Ben-Josef E, Griffith KA, Simeone D, Greenson JK, Francis IR, Hampton J, Colletti L, Chang AE, Lawrence TS, et al. Gemcitabine-based combination chemotherapy followed by radiation with capecitabine as adjuvant therapy for resected pancreas cancer. Int J Radiat Oncol Biol Phys. 2009; 75:1450–1455. [PubMed: 19409732]

Dingli DMF, Antal T, Pacheco JM. The emergence of tumor metastases. Cancer Biol Ther. 2007; 6:383–390. [PubMed: 17312385]

Embuscado EELD, Ricci F, Yun KJ, de Boom Witzel S, Seigel A, Flickinger K, Hidalgo M, Bova GS, Iacobuzio-Donahue CA. Immortalizing the complexity of cancer metastasis: genetic features of lethal metastatic pancreatic cancer obtained from rapid autopsy. Cancer Biol Ther. 2005; 4:548–554. [PubMed: 15846069]

Haeno H, Michor F. The evolution of tumor metastases during clonal expansion. J Theor Biol. 2011; 263:30–44. [PubMed: 19917298]

Hahn SA, Schutte M, Hoque AT, Moskaluk CA, da Costa LT, Rozenblum E, Weinstein CL, Fischer A, Yeo CJ, Hruban RH, et al. DPC4, a candidate tumor suppressor gene at human chromosome 18q21.1. Science. 1996; 271:350–353. [PubMed: 8553070]

Hidalgo M. Pancreatic cancer. N Engl J Med. 2010; 362:1605–1617. [PubMed: 20427809]

Hruban RH, Goggins M, Parsons J, Kern SE. Progression model for pancreatic cancer. Clin Cancer Res. 2000; 6:2969–2972. [PubMed: 10955772]

Hsu CC, Herman JM, Corsini MM, Winter JM, Callister MD, Haddock MG, Cameron JL, Pawlik TM, Schulick RD, Wolfgang CL, et al. Adjuvant chemoradiation for pancreatic adenocarcinoma: the Johns Hopkins Hospital-Mayo Clinic collaborative study. Ann Surg Oncol. 2010; 17:981–990. [PubMed: 20087786]

Iacobuzio-Donahue CA. Genetic evolution of pancreatic cancer: lessons learnt from the pancreatic cancer genome sequencing project. Gut. 2011

Iacobuzio-Donahue CAFB, Yachida S, Luo M, Abe H, Henderson CM, Vilardell F, Wang Z, Keller JW, Banerjee P, Herman JM, Cameron JL, Yeo CJ, Halushka MK, Eshleman JR, Raben M, Klein AP, Hruban RH, Hidalgo M, Laheru D. DPC4 gene status of the primary carcinoma correlates with patterns of failure in patients with pancreatic cancer. J Clin Oncol. 2009; 27:1806–1813. [PubMed: 19273710]

Jadhav S, Eggleton CD, Konstantopoulos K. Mathematical modeling of cell adhesion in shear flow: application to targeted drug delivery in inflammation and cancer metastasis. Curr Pharm Des. 2007; 13:1511–1526. [PubMed: 17504147]

Jemal ASR, Xu J, Ward E. Cancer statistics, 2010. CA Cancer J Clin. 2010; 60:277–300. [PubMed: 20610543]

Jones S, Zhang X, Parsons DW, Lin JC, Leary RJ, Angenendt P, Mankoo P, Carter H, Kamiyama H, Jimeno A, et al. Core signaling pathways in human pancreatic cancers revealed by global genomic analyses. Science. 2008; 321:1801–1806. [PubMed: 18772397]

Katz MH, Wang H, Fleming JB, Sun CC, Hwang RF, Wolff RA, Varadhachary G, Abbruzzese JL, Crane CH, Krishnan S, et al. Long-term survival after multidisciplinary management of resected pancreatic adenocarcinoma. Ann Surg Oncol. 2009; 16:836–847. [PubMed: 19194760]

Klein CA, Holzel D. Systemic cancer progression and tumor dormancy: mathematical models meet single cell genomics. Cell Cycle. 2006; 5:1788–1798. [PubMed: 16929175]

Lengauer CKK, Vogelstein B. Genetic instability in colorectal cancers. Nature. 1997; 386:623–627. [PubMed: 9121588]

Lengauer CKK, Vogelstein B. Genetic instabilities in human cancers. Nature. 1998; 396:643–649. [PubMed: 9872311]

Liu WLS, Khan S, Vihinen M, Kowalski J, Yu G, Chen L, Ewing CM, Eisenberger MA, Carducci MA, Nelson WG, Yegnasubramanian S, Luo J, Wang Y, Xu J, Isaacs WB, Visakorpi T, Bova GS. Copy number analysis indicates monoclonal origin of lethal metastatic prostate cancer. Nat Med. 2009; 15:559–565. [PubMed: 19363497]

Lu X, Kang Y. Hypoxia and hypoxia-inducible factors: master regulators of metastasis. Clin Cancer Res. 2010; 16:5928–5935. [PubMed: 20962028]

Luzzi KJMI, Schmidt EE, Kerkvliet N, Morris VL, Chambers AF, Groom AC. Multistep nature of metastatic inefficiency: dormancy of solitary cells after successful extravasation and limited survival of early micrometastases. Am J Pathol. 1998; 153:865–873. [PubMed: 9736035]

Michor FNM, Iwasa Y. Stochastic dynamics of metastasis formation. J Theor Biol. 2006; 240:521–530. [PubMed: 16343545]

Neoptolemos JPSD, Friess H, Bassi C, Dunn JA, Hickey H, Beger H, Fernandez-Cruz L, Dervenis C, Lacaine F, Falconi M, Pederzoli P, Pap A, Spooner D, Kerr DJ, Büchler MW. European Study Group for Pancreatic Cancer. A randomized trial of chemoradiotherapy and chemotherapy after resection of pancreatic cancer. N Engl J Med. 2004; 350:1200–1210. [PubMed: 15028824]

Neuhaus PRH, Post S. CONKO-001: Final results of the randomized, prospective, multicenter phase III trial of adjuvant chemotherapy with gemcitabine versus observation in patients with resected pancreatic cancer (PC). J Clin Oncol. 2008; 26:214s. (suppl; abstr LBA4504).

Nguyen DX, Bos PD, Massague J. Metastasis: from dissemination to organ-specific colonization. Nat Rev Cancer. 2009; 9:274–284. [PubMed: 19308067]

Nguyen DXMJ. Genetic determinants of cancer metastasis. Nat Rev Genet. 2007; 8:341–352. [PubMed: 17440531]

Oettle HPS, Neuhaus P, Gellert K, Langrehr J, Ridwelski K, Schramm H, Fahlke J, Zuelke C, Burkart C, Gutberlet K, Kettner E, Schmalenberg H, Weigang-Koehler K, Bechstein WO, Niedergethmann M, Schmidt-Wolf I, Roll L, Doerken B, Riess H. Adjuvant chemotherapy with gemcitabine vs observation in patients undergoing curative-intent resection of pancreatic cancer: a randomized controlled trial. JAMA. 2007; 297:267–277. [PubMed: 17227978]

Polyak KWR. Transitions between epithelial and mesenchymal states: acquisition of malignant and stem cell traits. Nat Rev Cancer. 2009; 9:265–273. [PubMed: 19262571]

Quaranta V, Rejniak KA, Gerlee P, Anderson AR. Invasion emerges from cancer cell adaptation to competitive microenvironments: quantitative predictions from multiscale mathematical models. Semin Cancer Biol. 2008; 18:338–348. [PubMed: 18524624]

Saha SBA, Buckhaults P, Velculescu VE, Rago C, StCroix B, Romans KE, Choti MA, Lengauer C, Kinzler KW, Vogelstein B. A phosphatase associated with metastasis of colorectal cancer. Science. 2001; 294:1343–1346. [PubMed: 11598267]

Sato N, Goggins M. The role of epigenetic alterations in pancreatic cancer. J Hepatobiliary Pancreat Surg. 2006; 13:286–295. [PubMed: 16858539]

Schellenberg D, Kim J, Christman-Skieller C, Chun CL, Columbo LA, Ford JM, Fisher GA, Kunz PL, Van Dam J, Quon A, et al. Single-fraction stereotactic body radiation therapy and sequential gemcitabine for the treatment of locally advanced pancreatic cancer. Int J Radiat Oncol Biol Phys. 2011; 81:181–188. [PubMed: 21549517]

Seshadri RKR, Trainor K, Matthews C, Morley AA. Mutation rate of normal and malignant human lymphocytes. Cancer Res. 1987; 47:407–409. [PubMed: 3466691]

Shah RBMR, Chinnaiyan AM, Shen R, Ghosh D, Zhou M, Macvicar GR, Varambally S, Harwood J, Bismar TA, Kim R, Rubin MA, Pienta KJ. Androgen-independent prostate cancer is a heterogeneous group of diseases: lessons from a rapid autopsy program. Cancer Res. 2004; 64:9209–9216. [PubMed: 15604294]

Sherratt JA. Predictive mathematical modeling in metastasis. Methods Mol Med. 2001; 57:309–315. [PubMed: 21340907]

Stathis AMM. Advanced pancreatic carcinoma: current treatment and future challenges. Nat Rev Clin Oncol. 2010; 7:163–172. [PubMed: 20101258]

Stephens PJ, Greenman CD, Fu B, Yang F, Bignell GR, Mudie LJ, Pleasance ED, Lau KW, Beare D, Stebbings LA, et al. Massive genomic rearrangement acquired in a single catastrophic event during cancer development. Cell. 2011; 144:27–40. [PubMed: 21215367]

Talmadge JEFI. AACR centennial series: the biology of cancer metastasis: historical perspective. Cancer Res. 2010; 70:5649–5669. [PubMed: 20610625]

Valastyan SBN, Chang A, Reinhardt F, Weinberg RA. Concomitant suppression of three target genes can explain the impact of a microRNA on metastasis. Genes Dev. 2009; 23:2592–2597. [PubMed: 19875476]

van Heek NT, Meeker AK, Kern SE, Yeo CJ, Lillemoe KD, Cameron JL, Offerhaus GJ, Hicks JL, Wilentz RE, Goggins MG, et al. Telomere shortening is nearly universal in pancreatic intraepithelial neoplasia. Am J Pathol. 2002; 161:1541–1547. [PubMed: 12414502]

Yachida S, Jones S, Bozic I, Antal T, Leary R, Fu B, Kamiyama M, Hruban RH, Eshleman JR, Nowak MA, et al. Distant metastasis occurs late during the genetic evolution of pancreatic cancer. Nature. 2010; 467:1114–1117. [PubMed: 20981102]

HIGHLIGHTS

- A mathematical framework models pancreatic cancer progression
- The model allows characterization of growth and dissemination kinetics
- Treatment strategies to maximize patient survival are identified

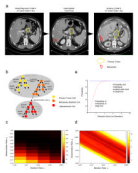

Figure 1. A mathematical framework of pancreatic cancer progression allows the prediction of growth and dissemination kinetics

(a) Computed tomography (axial view) of one representative patient at initial diagnosis, one intermediate time point five months later, and then again at 7 months after diagnosis, which was also one week before death. In each image the primary pancreatic cancer is indicated in dashed yellow outlines and the liver metastases by dashed red outlines. (b) The mathematical framework. The model considers three cell types: type-0 cells, which have not yet evolved the ability to metastasize, reside in the primary tumor where they proliferate and die at rates r and d. They give rise to type-1 cells at rate u per cell division; these cells have evolved the ability to metastasize but still reside in the primary tumor, where they proliferate and die at rates a_1 and b_1, respectively, and disseminate to a new metastatic site at rate q per time unit. Once disseminated, cells are called type-2 cells and proliferate and die at rates a_2 and b_2, respectively. This mathematical framework can be used to determine quantities such as the risk of metastatic disease at diagnosis and the expected number of metastasized cells at death. (c and d) Estimated mutation and dissemination rates allow the prediction of the probability of metastasis at diagnosis. The color represents the deviations between the data and the results of the mathematical model; we used patient data on the number of metastatic sites and metastatic cells for the estimation, and then calculated the geometric mean of the two values for each point. Darker colors represent the region of fit between theory and data. Panel d provides a more detailed analysis of the data shown in panel c. (e) The panel shows the probability of metastasis at diagnosis (red curve) and the probability of the existence of cells in the primary tumor that have evolved the potential to metastasize (blue curve). Parameters are $u = 6.31 \cdot 10^{-5}$, $q = 6.31 \cdot 10^{-7}$, $r = a_1 = 0.16$, $a_2 = 0.58$, $d = b_1 = 0.01r$, and $b_2 = 0.01a_2$.

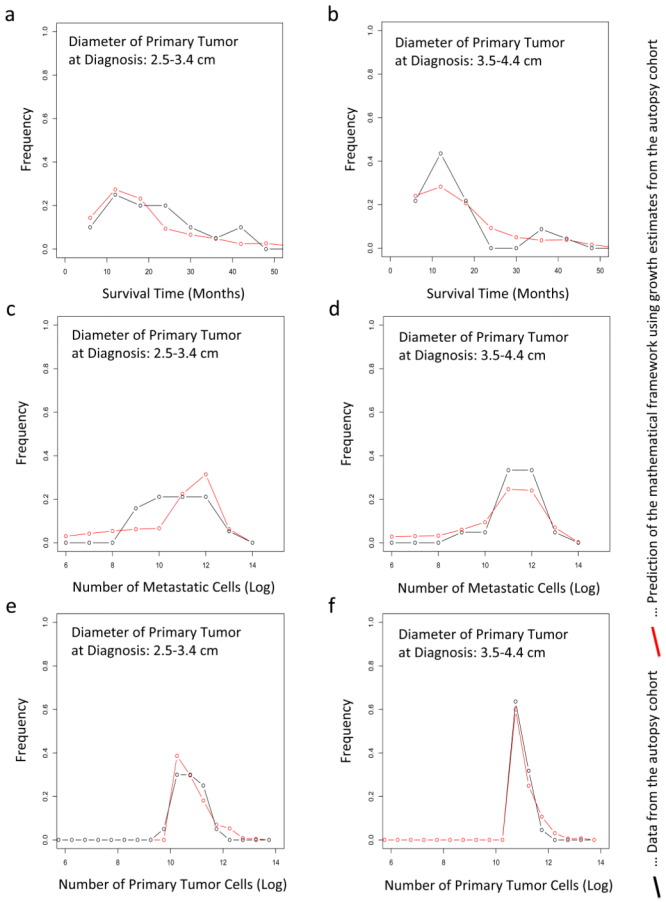

Figure 2. The predictions of the mathematical framework are validated using patient data

(a and b) The panels show the distribution of survival times of patients who were diagnosed with primary tumors with a diameter of 2.5 – 3.4 cm (panel a) and of 3.5 – 4.4 cm (panel b). (c–d) The panels show the distribution of the number of metastatic cells at autopsy of patients who were diagnosed with primary tumors with a diameter of 2.5 – 3.4 cm (panel c) and of 3.5 – 4.4 cm (panel d). (e–f) The panels show the distribution of the number of primary tumor cells at autopsy of patients who were diagnosed with primary tumors with a diameter of 2.5 – 3.4 cm (panel e) and of 3.5 – 4.4 cm (panel f). In all panels, the red curves represent the prediction of the mathematical framework and the black lines represent the data. We observed no significant difference between the predictions and the data; the p-values are (a) 0.26, (b) 0.63, (c) 0.54, (d) 0.47, (e) 0.13, and (f) 0.11. Parameters are $u = 6.31 \cdot 10^{-5}$, $q = 6.31 \cdot 10^{-7}$, $d = b_1 = 0.01r$, $b_2 = 0.01a_2$ and $\gamma = 0.7$. Tumor size at autopsy was obtained from the normal distribution with mean 11.2 and variance 0.46 in a base 10 logarithmic scale for each calculation. The growth rate of primary tumor cells and metastatic tumor cells are obtained from the normal distribution with mean 0.16 and variance 0.14, and mean 0.58 and variance 2.72, respectively.

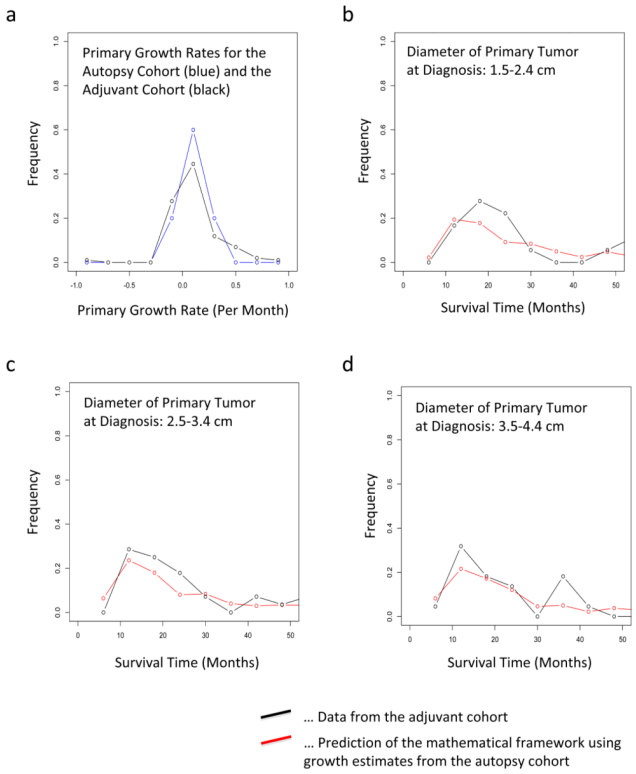

Figure 3. Validation of our framework using an independent patient cohort

(a) The distribution of the primary growth rate from the original dataset including 101 patients is shown in red and that from the additional data in black; for the latter, only 10 patients had sufficient follow-up measurements (size at diagnosis, intermediate, and death) such that the growth rate could be determined. (b) The panel shows the distribution of survival times of patients after resection of the primary tumor with 2 (1.5–2.4) cm diameter after diagnosis. The red curve represents the prediction of the mathematical framework and the black line represents the data. (c) The panel shows the distribution of survival times of patients after resection of the primary tumor with 3 (2.5–3.4) cm diameter after diagnosis. The red curve represents the prediction of the mathematical framework and the black line represents the data. (d) The panel shows the distribution of survival times of patients after resection of the primary tumor with 4 (3.5–4.4) cm diameter after diagnosis. The red curve represents the prediction of the mathematical framework and the black line represents the data. We observed no significant difference between the predictions and the data; the p-values are (a) 0.45, (b) 0.44, (c) 0.40, and (d) 0.41. Parameters used are $u = 6.31 \cdot 10^{-5}$, $q = 6.31 \cdot 10^{-7}$, $d = b_1 = 0.01r$, $b_2 = 0.01a_2$ and $\gamma = 0.7$. Tumor size was obtained from a normal distribution with mean 11.2 and variance 0.46 in a base 10 logarithmic scale for each calculation. The growth rate of primary tumor cells and metastatic tumor cells were obtained from a normal distribution with mean 0.16 and variance 0.14, and mean 0.58 and variance 2.72, respectively.

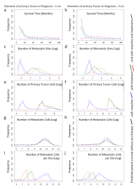

Figure 4. The mathematical framework predicts optimum treatment strategies for pancreatic cancer patients

The panels show the predictions of different quantities for a tumor size of 1 cm diameter at diagnosis (left column) and 3 cm at diagnosis (right column). The tumor size at autopsy in a 10 base logarithmic scale was obtained from a normal distribution with mean 11.2 and variance 0.46 for each calculation. The growth rates of primary tumor cells and metastatic tumor cells were obtained from a normal distribution with mean 0.16 and variance 0.14; and mean 0.58 and variance 2.72, respectively. The black curve represents mathematical predictions of the survival time without treatment or resection, the blue curve with resection (removal of 99.99% of the primary tumor by surgery), the red and green curves with treatment (90% (red) and 50% (green) reduction of the growth rate), and purple curve with resection and treatment (removal of 99.99% of the primary tumor by surgery and 90% reduction of the growth rate). Parameters are $u = 6.31 \cdot 10^{-5}$, $q = 6.31 \cdot 10^{-7}$, $d = b_1 = 0.01r$, $b_2 = 0.01a_2$, $\varepsilon = 0.9999$, and $\gamma = 0.9$ (red and purple curve) and $\gamma = 0.5$ (green curve). (a and b) Survival time. (c and d) The number of metastatic sites at autopsy. (e and f) The number of primary tumor cells. (g and h) The number of metastatic tumor cells. (i and j) The number of metastatic tumor cells per site. See also Figure S2–S7.

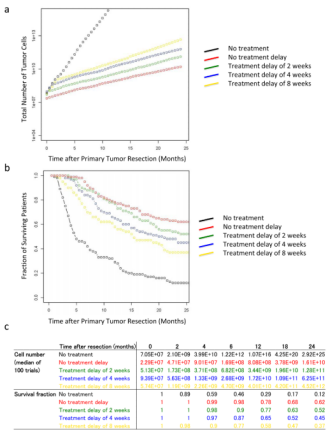

	Time after resection (months)	0	2	4	6	12	18	24
Cell number (median of 100 trials)	No treatment	7.05E+07	2.10E+09	3.98E+10	1.22E+12	1.07E+16	4.25E+20	2.92E+25
	No treatment delay	2.39E+07	4.71E+07	9.01E+07	1.89E+08	8.08E+08	3.78E+09	1.61E+10
	Treatment delay of 2 weeks	5.13E+07	1.72E+08	3.71E+08	6.82E+08	3.44E+09	1.90E+10	1.20E+11
	Treatment delay of 4 weeks	9.39E+07	5.63E+08	1.33E+09	2.68E+09	1.72E+10	1.09E+11	6.25E+11
	Treatment delay of 8 weeks	1.96E+08	2.29E+09	4.29E+09	1.05E+10	6.66E+11	4.20E+12	
Survival fraction	No treatment	1	0.89	0.59	0.46	0.29	0.17	0.12
	No treatment delay	1	1	0.99	0.98	0.76	0.65	0.62
	Treatment delay of 2 weeks	1	1	0.98	0.9	0.77	0.63	0.52
	Treatment delay of 4 weeks	1	1	0.97	0.87	0.65	0.52	0.45
	Treatment delay of 8 weeks	1	1.00	0.9	0.77	0.56	0.47	0.39

Figure 5. A delay in the initiation of therapy significantly increases tumor volume and shortens survival

The panels show the prognosis after surgery with different theoretical treatment options and treatment delays. Panel a shows the median of the number of tumor cells in 100 trials over time. Panel b shows the fraction of surviving patients in 100 trials at each time point. Panel c shows the numbers of tumor cells and the fraction of surviving patients. The tumor size at autopsy was obtained from a normal distribution with mean 11.2 and variance 0.46 in a 10 base logarithmic scale. The growth rates of primary tumor cells and metastatic tumor cells were obtained from a normal distribution with mean 0.16 and variance 0.14; and mean 0.58 and variance 2.72, respectively. The black curve represents the case with no treatment after surgery, the red curve with starting treatment immediately after surgery, and the green, blue, and yellow curves with starting treatment 2, 4, and 8 weeks after surgery, respectively. Parameters are $u = 6.31 \cdot 10^{-5}$, $q = 6.31 \cdot 10^{-7}$, $d = b_1 = 0.01r$, $b_2 = 0.01a_2$, $\varepsilon = 0.9999$, and $\gamma = 0.7$.

Table 1

Summary of the patient cohorts

See also Table S1.

		Autopsy cohort	Adjuvant cohort
Total number of patients		101	127
Age*		64 (55–71)	61 (56–68)
Resected		26 (26%)	127 (100%)
Received adjuvant therapy	Yes	18 (18%)	127 (100%)
	No	12 (12%)	
	N/A	67 (67%)	
	Unknown	4 (4%)	
Received neoadjuvant therapy	Yes	2 (2%)	Unknown
	No	30 (30%)	
	N/A	65 (65%)	
	Unknown	1 (1%)	
Node-positive		Unknown	106 (85%)
Margin-positive		Unknown	50 (39%)
Stage I–III		70 (69%)	127 (100%)
Stage IV		31 (31%)	0 (0%)
Tumor size at diagnosis*		3.7 (2.8–4.2)	3 (2.5–4)
Progression-free survival*		8.4 (4.6 – 17.7)	12.8 (8.4 – 25.4)
Survival*		11.4 (6.1 – 24.4)	21.0 (13.2–46.4)

* shown as median (first and third quartiles)

Table 2

Correlations between various measures of tumor size and growth rate as well as survival in the autopsy cohort (101 patients)

See also Table S2 and Figure S1.

	Primary Size at Diagnosis	Met. Size at Diagnosis	Primary Size at Autopsy	Largest Met at Autopsy	Primary Growth Rate	Met. Growth Rate
Primary Size at Diagnosis	1.00					
Met. Size at Diagnosis	0.08	1.00				
Primary Size at Autopsy	0.36*	0.10	1.00			
Largest Met at Autopsy	−0.01	0.51*	0.01	1.00		
Primary Growth Rate	−0.04	0.10	0.28*	0.20*	1.00	
Met. Growth Rate	0.03	−0.15	−0.02	0.07	0.23*	1.00
Survival	−0.18	−0.45*	0.01	−0.14	−0.13	−0.32*

* $p < 0.05$